Electronic Supplementary Material (ESI) for Chemical Communications.

Tracking the super resolved structure of mitochondria using red emissive carbon nanodots as a fluorescent biomarker

Richa Garg[1,¥], Farhan Anjum[2,¥], Abdul Salam[1], Kush Kaushik[1], Shagun Sharma[1], Udisha Sahrawat[1], Aditya Yadav[1], and Chayan Kanti Nandi[1,]*

[1]School of Chemical Sciences, Indian Institute of Technology (IIT) Mandi, H. P.-175005, India.

[2]School of Biosciences and Bioengineering, Indian Institute of Technology (IIT) Mandi, H. P.-175005, India.

[¥]Richa Garg and Farhan Anjum equally contributed to this work

Supplementary Information

Materials and Methods:

All glassware and hydrothermal were washed with aqua regia (3HCl:1HNO3) and rinsed several times with double distilled water. Double-distilled (18.3 mΩ) deionized water (Elga Purelab Ultra, Vivendi water system Ltd, India) was used throughout the whole experimental process. o-Phenylenediamine, (*3*-Carboxypropyl)triphenylphosphonium bromide was purchased from Merck Chemicals. HCl was purchased from a local vendor. Dulbecco's Modified EagleMedium (DMEM), 1% Antibiotic-Antimicotic, Penstrap, and fetal bovine serum was purchased from Gibco. All chemicals were used without further purification. The cell lines (HeLa and HepG2) used in this study were purchased from the National Centre for Cell Science (NCCS) Complex, Pune, Maharashtra, India - 411 007.

Characterization

The UV-Vis of TPP-CNDs were recorded using a (50W halogen lamp (2000 h life)) Shimadzu UV-Vis 2450 spectrophotometer. For absorption spectra, samples were placed in a transparent quartz cuvette with 1 ml volume and 10 mm path length.

Steady-state fluorescence

Steady-state fluorescence was measured using a Horiba Fluorolog-3 spectrofluorometer from 280 to 600 nm in the excitation wavelength range.

Thermogravimetric Analysis (TGA)

Thermal properties were measured by Perkin Elmer Pyris Thermogravimetric (TGA) analyzer from room temperature to 800 °C with the heating rate of 10 °C min^{-1} under nitrogen atmosphere.

Transmission electron microscopy (TEM)

High-resolution images and particle morphology were observed by transmission electron microscopy (TEM) using FEI TECHNAI, USA, FP 5022/22-Tecnai G2 20 S-TWIN, that operates at 200 keV using tungsten filament as an excitation source.

Fourier transform infrared (FTIR) spectra

Fourier transform infrared (FTIR) spectra of dried samples were measured using a Perkin-Elmer FTIR spectrophotometer equipped with a horizontal attenuated total reflectance (ATR) accessory containing a zinc selenide crystal and operating at 4 cm^{-1} resolution. Spectrum was recorded using Resolutions Pro FTIR software by subtracting background spectra from the sample.

X-ray crystallography

Single-crystal X-ray diffraction data were collected on an Agilent SuperNova diffractometer, equipped with a dual source (Cu and Mo) and Eos charge-coupled device (CCD) detector, using Cu Kα radiation (1.541 84 Å) at 293 K. Data acquisition, reduction, and absorption correction were performed by using the CrysAlisPRO program. (67) The structures were solved by direct methods with ShelXS (68) and refined on F^2 by full-matrix least-squares techniques with ShelXL (68) using the Olex2 (v.1.2) program package. Figures and the publication data were generated using mercury (4.2.0) software.

Raman spectrum

The Raman spectrum was measured by the confocal microscope Raman spectrometer (Horiba Scientific, Xplo RA ONE) with 530 nm laser (spectral range 400cm^{-1} to 3500cm^{-1}.

NMR

^{1}H NMR spectra were recorded on a Jeol-ECX-500 MHz spectrometer using D2O as solvent and tetramethylsilane (TMS) as an internal standard. High-Resolution Mass spectral data were recorded using Bruker Daltonik GmbH impact-HD spectrometer.

AFM analysis

AFM analysis for particle size determination was carried out by using a digital instrument Bruker AFM (Dimension Icon-peak force tapping mode. Standard Veeco tapping mode silicon probes were used for scanning the sample.

X-Ray Photoelectron Spectroscopy (XPS)

Surface chemistry of the material and elemental composition is measured by using X-Ray Photoelectron Spectroscopy (XPS) in which Auger Electron Spectroscopy (AES) Module PHI 5000Versa Prob II, FEI Inc. and C_{60} sputter gun have been used for the characterization and scanning the spectra for C_{1S}, N_{1S}, O_{1S}, P_{1S} region.

Quantum yield

We have followed the standard methods and procedures for performing relative QY measurements. In our experiments, we first made dilutions of both the standard and sample solutions in PBS so that their absorbance spectra coincided at a particular wavelength (λ_{exc}). We then recorded the emission spectra for both TPP CNDs and Cy 5 dye solutions at λ_{exc}. This step was repeated for 5 dilutions. Then the emission spectrum was taken for both reference (Cy 5) and sample (CNDs) by exciting the solution from the previous step at λ_{exc}=625 nm (intersecting point). Now the area under the curve of the emission for each concentration was calculated one by one. The area under the curve calculation via Origin Pro software is shown below in **Fig. S8a**.

A scatter plot was then plotted for integrated fluorescence intensity vs. absorbance for all of the dilutions of the sample and standard solutions. The plots were then linearly fitted. The slopes of the fitted lines were noted as shown in **Fig. S8a, b.**

The reported quantum yield for Reference (Cy 5) is 27%. The quantum yield of the sample was then calculated using the following equation:

$$QY_{Sample} = QY_{Standard} \times \left(\frac{Slope\ for\ sample}{Slope\ for\ Standard}\right) \times \left(\frac{\eta^2_{sample}}{\eta^2_{Standard}}\right)$$

where η is the refractive index of the solution.

This yields the quantum yield of TPP CNDs to be 16 %. Also, the measurement was repeated three times to get a precise value. Special care was taken to ensure that the absorbance of the sample was kept below 0.1 in all cases, in order to avoid any unnecessary concentration effects or inner filter effects.

Confocal Imaging of HeLa Cells

Coverslip preparation: The glass slides and coverslips were cleaned by incubating in freshly prepared Piranha solution for 30 min and finally washing with MiliQ water in bath sonication, then dried under nitrogen.

Cell Culture, fixation, and staining: All the cell culture experiments and slide preparations were performed under the compliance with the relevant guidelines and norms of biosafety level-1 requirements of the Indian Institute of Technology Mandi. Cell lines were maintained by following the recommended protocols of the National Centre for Cell Science (NCCS) Complex, Pune, Maharashtra, India - 411 007.

Human cancer cell lines **(**HeLa cells) were grown as per recommendation in Dulbecco's

Modified EagleMedium (DMEM) with 10% fetal bovine serum with 1% anti-anti and penstrap at 37^{o}C with 5 % CO_2. HepG2 cells were also grown in the same DMEM media with 10% fetal bovine serum along with 1% anti-anti and penstrap. The cells were grown in a 6-well plate on coverslips with 10^4 cells per 100 µl density. Each well was filled with 2 ml of growth medium, and the cells were allowed to grow overnight for proper adherence and growth. An optical microscope examined the cells' growth and attachment to the coverslips. Once the cells reached the proper adherence and confluency, they were stained with synthesized TPP CNDs material to achieve enough labeling density for confocal microscopy. Finally, the cells were fixed by incubating with 4% paraformaldehyde solution in 1x PBS buffer for 15 min. The fixed cells were then washed 2-3 times with PBS buffer to remove extra TPP CNDs and Cell culture medium. The coverslips were fixed on a glass slide before imaging. For Hyperglycemic conditions, HepG2 cells were maintained in DMEM media, with 1% antibiotic and 10% FBS, to mimic the hyperglycaemic condition we supplemented high glucose (30mM) into the media and exposed the cells into high glucose medium for 48 hrs by following the protocol [1]

ROS detection: ROS detection was achieved by seeding the cells (40 X 10^3 cells per well), after the proper adherence of cells, they were incubated with CND for 24 hrs. After the incubation, 1uM of H_2DCFDA was added to the cell medium and incubated for 30 minutes. Finally, the fluorescence intensity of cells was measured at 520 nm after excitation with 490 nm, identification of ROS was achieved and compared with the control sample.

Cell cytotoxicity: Cell cytotoxicity was detected with the help of XTT kit (Roche XTT kit II), for this cells were seeded into 96 well plate with density of 4 X 10^3. Then incubated with TPP CNDs for 2 hrs, at 37°C in CO_2 incubator. After the incubation XTT labelling mixture was added and further incubated for 12-16 hours, at 37^{o}C in CO_2 incubator. Then absorbance of the sample mixture was taken by microplate reader at 550 nm of wavelength. The reference wavelength was set at 650 nm and then analyzed the cell viability against TPP CNDs with comparison to blank and control samples.

Confocal microscopy: Confocal imaging of HeLa cells was performed using Nikon Eclipse Ti inverted microscope and images were acquired using Nikon Nis-Element software. The cell samples were excited by using 560 nm laser. Finally, the images were collected by choosing a proper filter set.

SRRF Imaging

The recorded movie of 2000 frames was analyzed with an open-source version of the Nano-SRRF ImageJ plugin software. The SRRF analysis was optimized and obtained at the ring radius of 0.5, radiality magnification 5, ring in axis 6. Before SRRF analysis, drift correction was done using the NanoJ core ImageJ plugin. The background was determined from the image region in which no signal was present at the measurement time. To get a background-free signal, the mean value of this background was removed from the original trajectory. The open-source ImageJ NanoJ SRRF plugin was used to process the data. To get the ultrastructural detailed images of mitochondria labeled by the TPP CNDs, we carried SRRF microscopy with the help of two of our setups, (1) is a custom-built setup equipped with 100× Plan Apo objective (Nikon), an electron-multiplying charge-coupled device camera (EMCCD) to capture the images and videos upon excitation by a 532 nm laser. (2) other setup is commercial confocal microscope setup equipped with fluorescent lamp with various filter sets. The EMCCD captured a movie consisting of 2000 frames, each with an acquisition time of from 0.02-0.05 seconds. The recorded movie was anaysed with NanoJ-SRRF, a plug-in of ImageJ using a high-performance GPU (NVIDIA GeForce RTX 3070). Background correction was done using NanoJ-SRRF plugin.

Synthesis of TPP CNDs:

CNDs were synthesized via a simple facile hydrothermal method utilizing (3-Carboxypropyl) triphenylphosphonium bromide (TPP) and o-Phenylenediamine (OPDA) as precursors. Briefly, 0.108 g TPP and OPDA precursors were mixed in 10 ml of deionized water (DI) and 2 ml of 5% hydrochloric acid (HCl) solution. The mixture was stirred, sonicated for 15 minutes and infused into a 100 ml hydrothermal reactor. The solution was heated at 180° C for 12 h. After completion of the reaction, the mixture was cooled at room temperature. Further, the obtained reaction product was centrifuged at 3000 rpm for 30 minutes to remove unwanted impurities. Dialysis was then performed against DI water to obtain a pure sample of TPP CNDs. The solid sample was then obtained by freeze-drying.

Supplementary figures

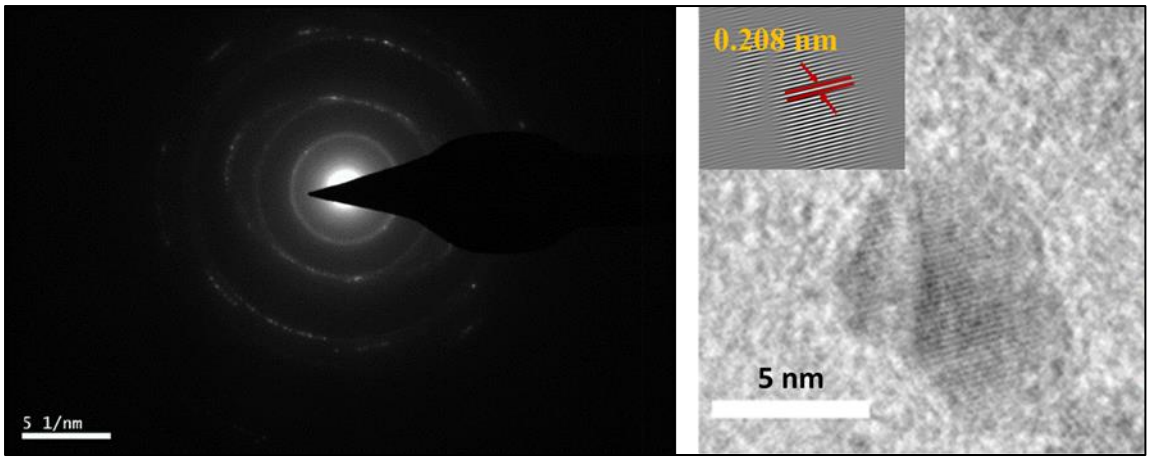

Fig. S1: SAED pattern confirms the polycrystalline nature of the TPP CNDs and HRTEM illustrating the carbon core. The fringes (right-hand side) confirm the graphitic planes.

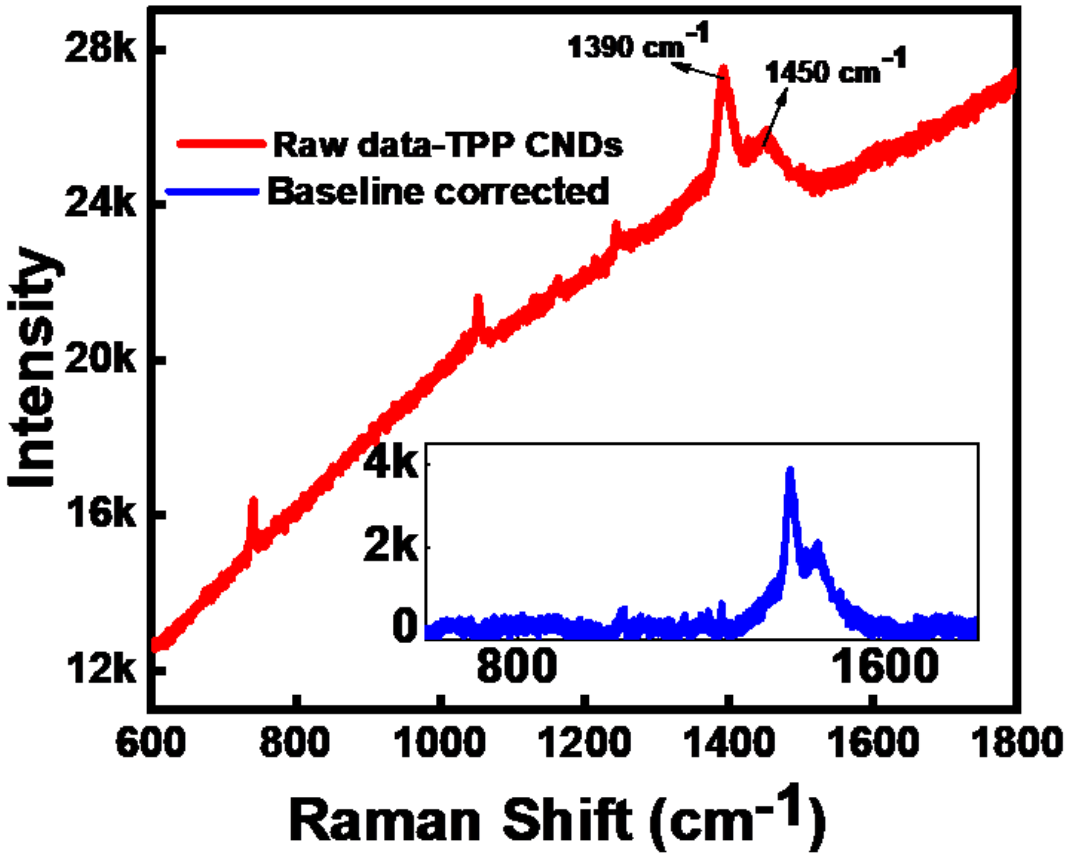

Fig. S2: Raman spectra of the TPP CNDs when excited with 532 nm laser. The D & G bands were appeared at 1390 cm^{-1} (D-band) and 1450 cm^{-1} (G-band) over the fluorescence envelop. The deconvoluted data (inset) showed the real D & G bands.

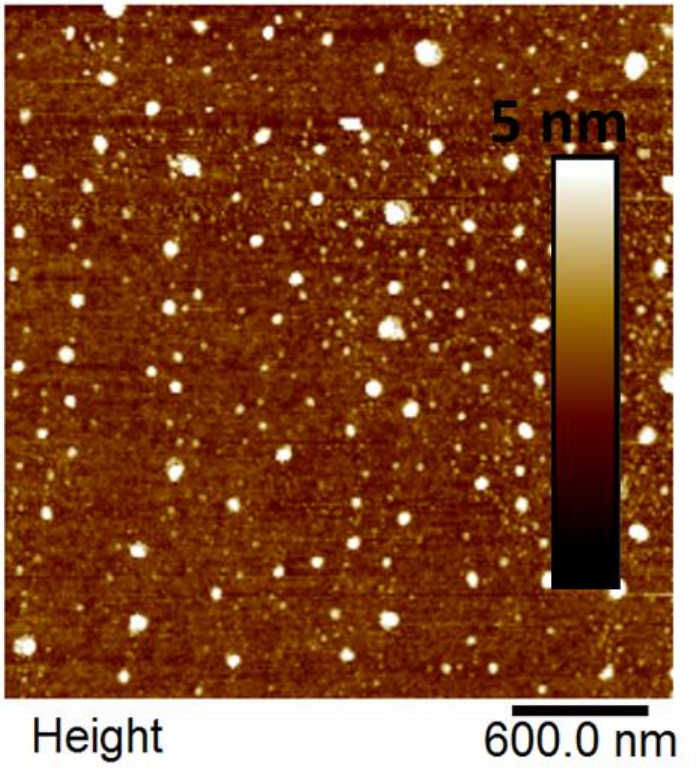

Fig. S3: AFM image with an average height profile of ~5 nm

		Mean (mV)	Area (%)	St Dev (mV)
Zeta Potential (mV): 18.5	**Peak 1:**	18.5	100.0	11.1
Zeta Deviation (mV): 11.1	**Peak 2:**	0.00	0.0	0.00
Conductivity (mS/cm): 4.29	**Peak 3:**	0.00	0.0	0.00
Result quality : Good				

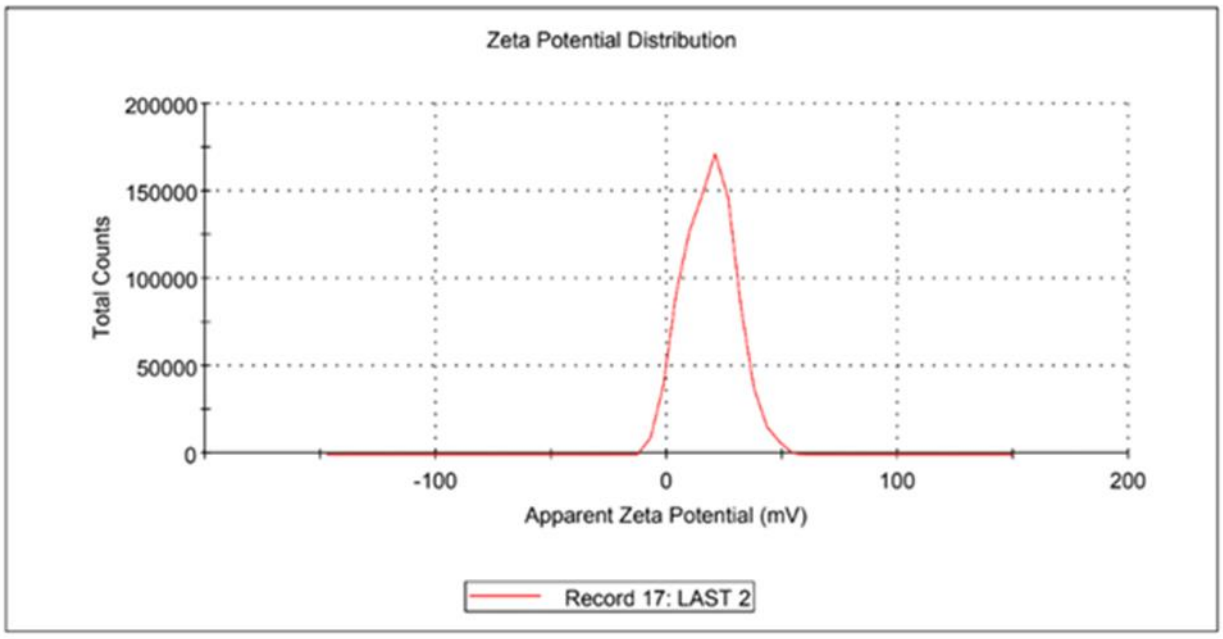

Fig. S4: Zeta potential of TPP CNDs with a value of +18.5 mV.

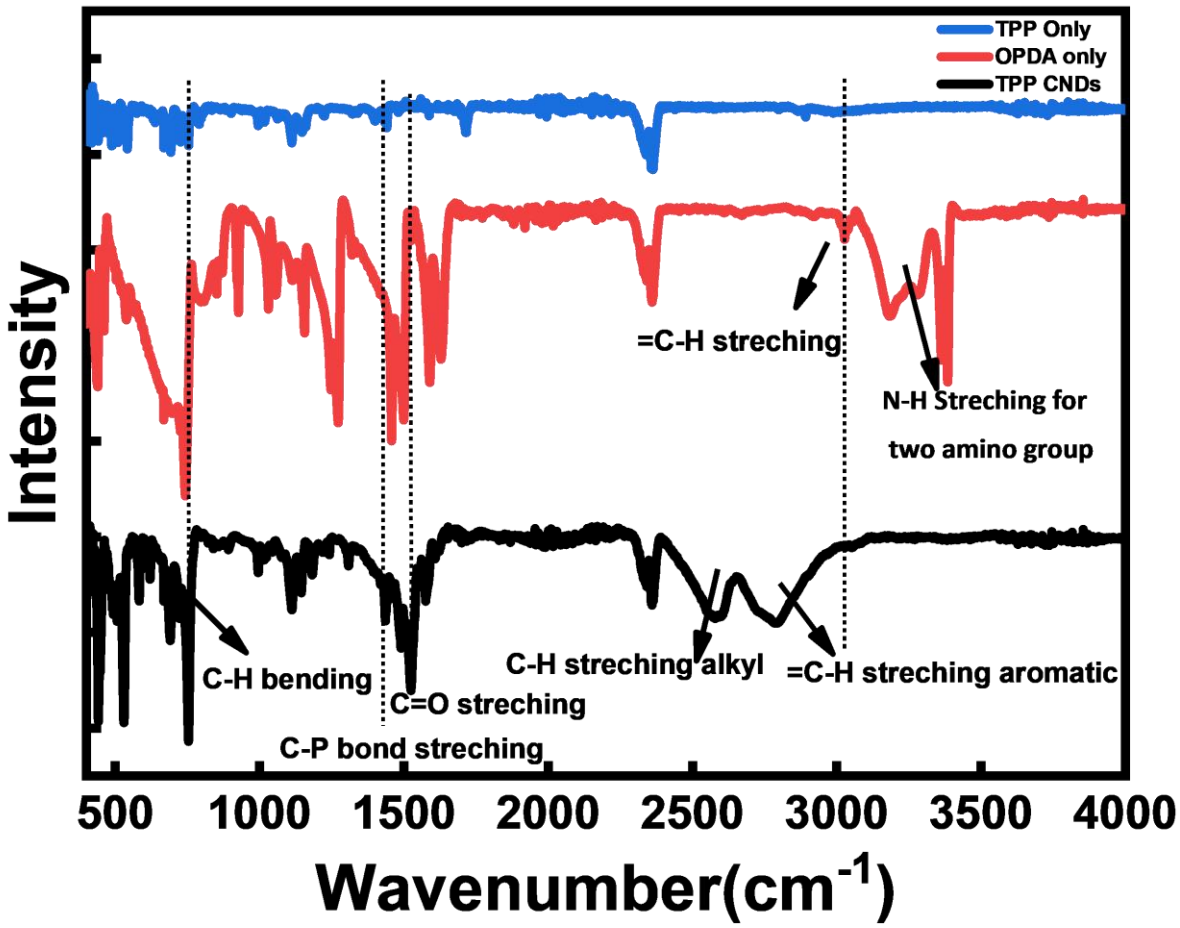

Fig. S5: FTIR spectrum of TPP, OPDA, and TPP CNDs in 500-4000 cm^{-1} region. The formation of TPP CNDs is clearly visible from the changes in the FTIR spectra.

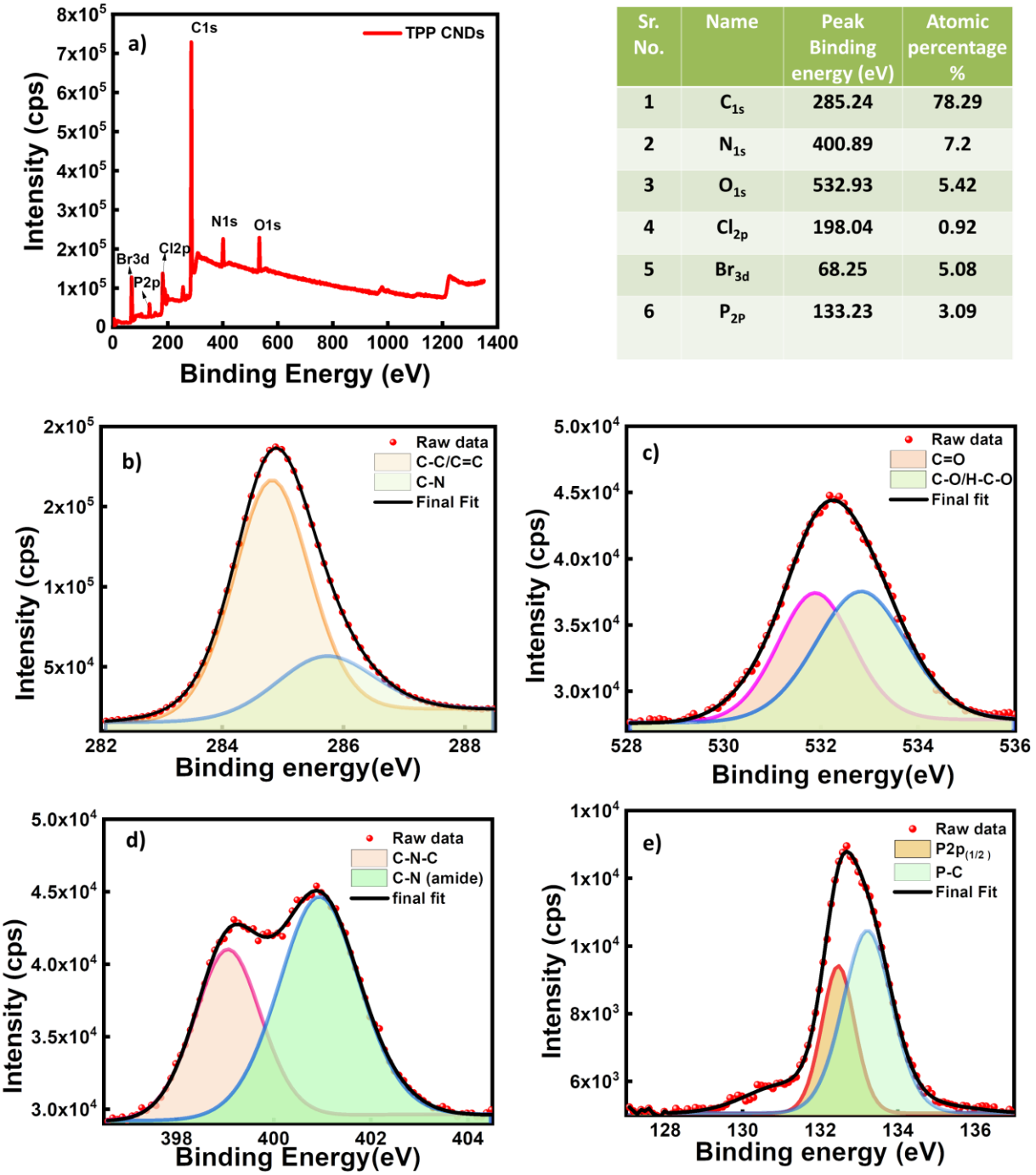

Sr. No.	Name	Peak Binding energy (eV)	Atomic percentage %
1	C_{1s}	285.24	78.29
2	N_{1s}	400.89	7.2
3	O_{1s}	532.93	5.42
4	Cl_{2p}	198.04	0.92
5	Br_{3d}	68.25	5.08
6	P_{2P}	133.23	3.09

Fig. S6: a) The XPS survey of TPP CNDs. The Deconvoluted spectra of b) C1s, c) O1s, d) N1s and e) P2p. The XPS data showed that TPP CNDs mainly contained C (78.29 atomic %), O (5.42 atomic %), P (3.09 atomic %), and N (7.2 atomic %). The C 1s deconvolution shows peaks at 285.7 and 284.83 eV, corresponding to the binding energy of C-C/C=C and C-N groups, respectively. The O1s deconvolution spectrum could be fitted into two components corresponding to oxygen states of C-O/C=O at 532.8 eV and C=O at 531eV. The N 1s deconvolution spectrum could be split into two different peaks at 400.94, and 399.07 eV which are arising from C-N and C-N-C groups. The P1s deconvolution spectrum of TPP CNDs contains two peaks at 132.5 eV and 133.2 eV corresponding to $P2P_{(1/2)}$, and P-C, respectively.

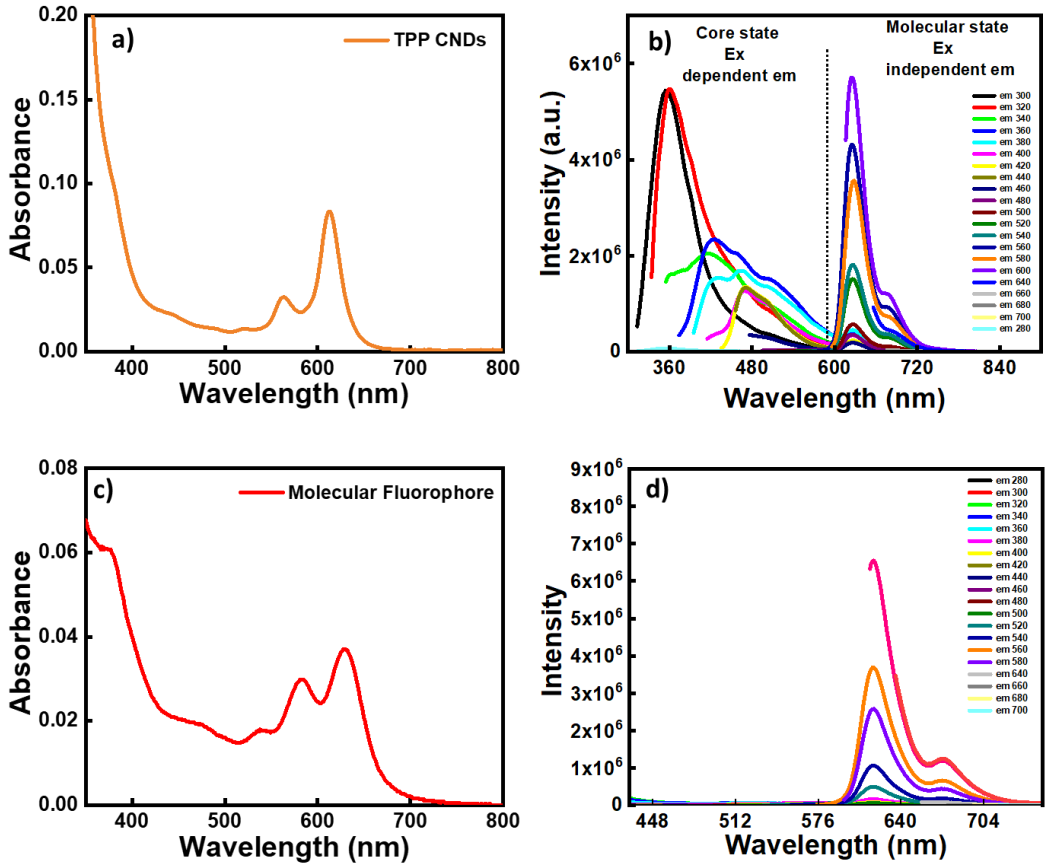

Fig. S7: (a) UV Visible absorption spectrum of TPP CNDs, (b) emission spectrum of TPP CNDs, (c) UV Visible absorption spectrum of molecular fluorophore, and (d) emission spectrum of molecular fluorophore.

a)

625 Exc	Absorbance	Area Under the Curve	
		Cy 5	TPP CNDs
Conc - 1	0.039	1133.85	804.15
Conc - 2	0.046	1383.79	1094.59
Conc - 3	0.06	1991.50	1432.35
Conc - 4	0.073	2680.01	1850.33
Conc - 5	0.086	3450.31	2078.22

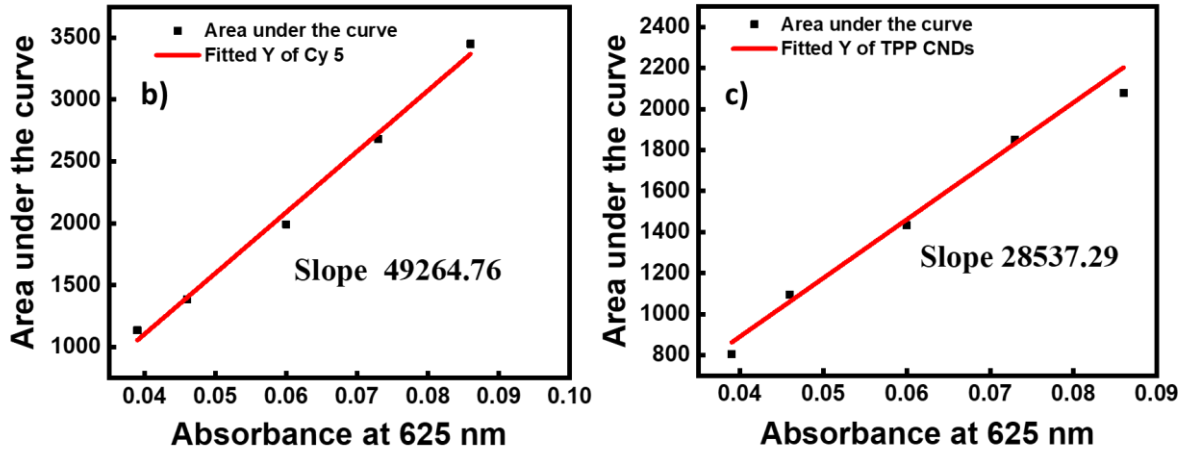

Fig. S8: (a) Recorded absorbance values and area under the curve values for five concentrations of Cy 5 dye and TPP CNDs in PBS. Plot obtained with area under the curve on y-axis and absorbance at x-axis for (b) Cy 5 and for (c)TPP CNDs. The solid red line represents the linear fit. The slope of these curves are noted down and used in final calculation.

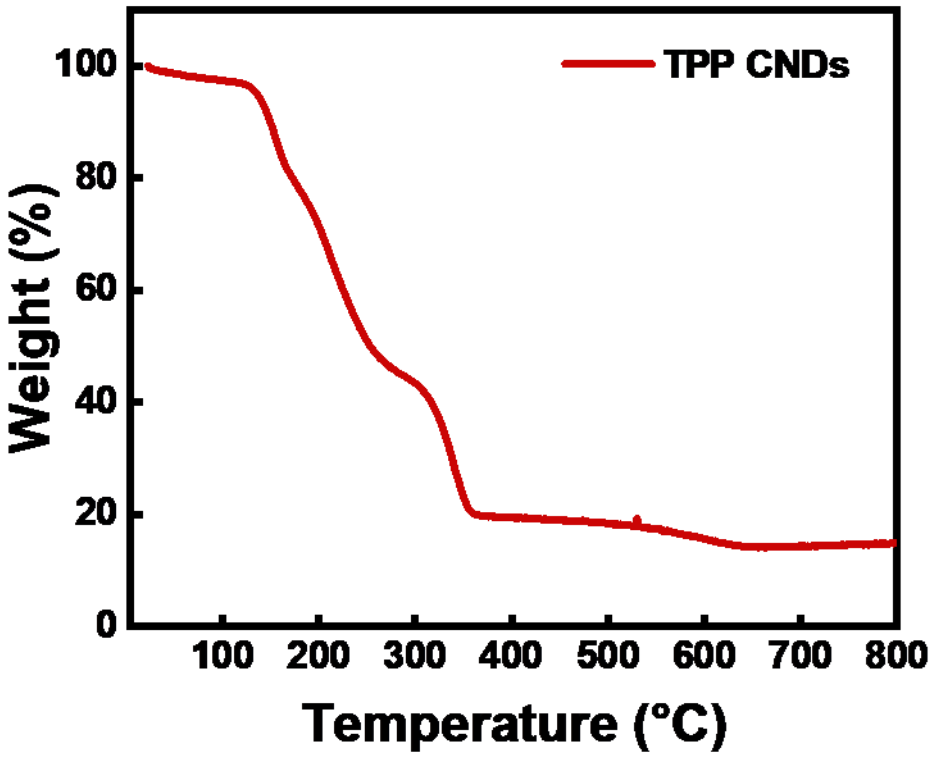

Fig. S9: Thermogravimetric analysis of TPP CNDs containing molecular fluorophores. The mass loss at 150 ˚C to 250 ˚C and from 250 ˚C to 360 ˚C confirms the presence of molecular fluorophore.

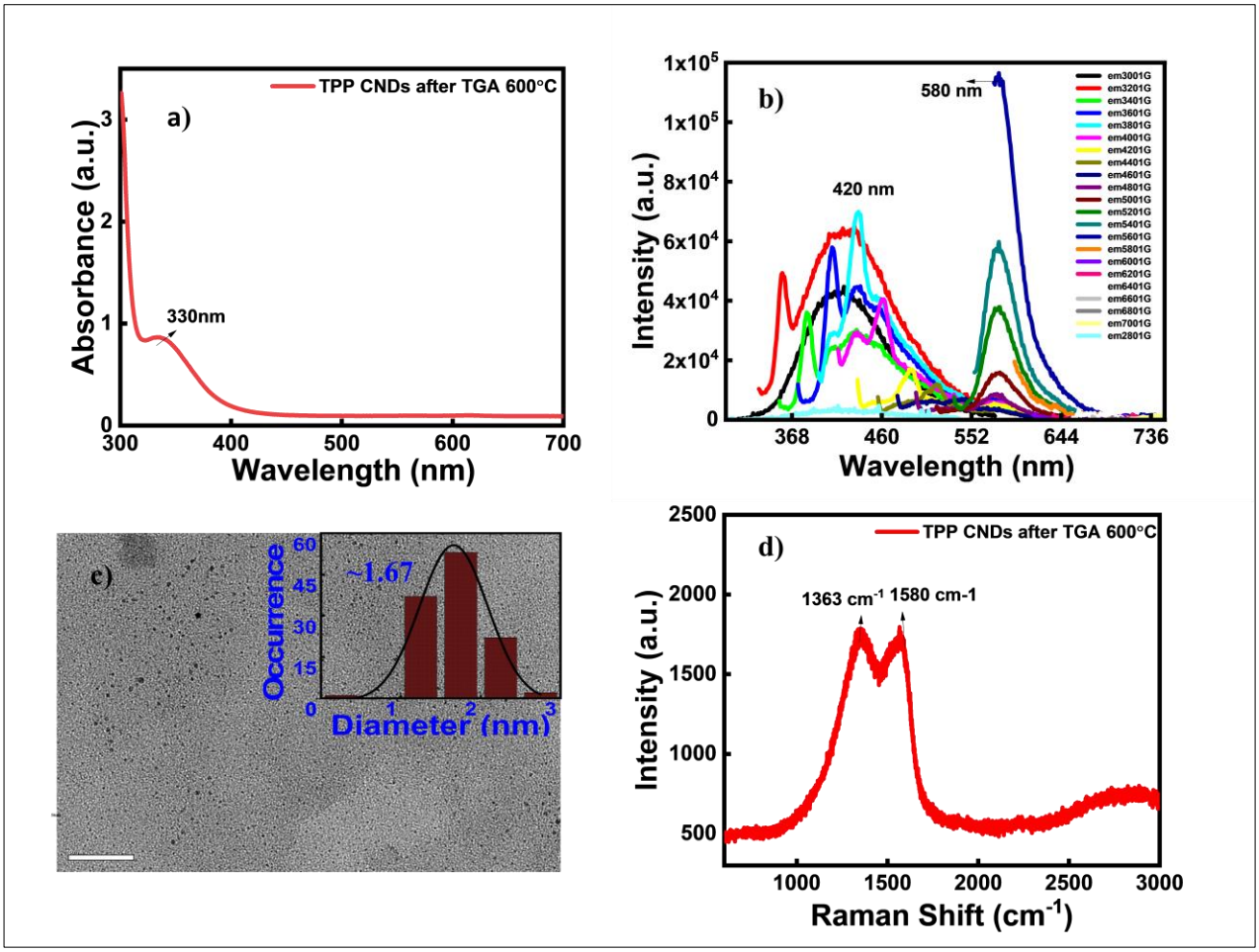

Fig. S10: (a) Absorption, (b) Emission, (c) TEM, and (c) Raman spectra of TPP CNDs after TGA treatment.

X-ray crystallographic data for Molecular Fluorophore

The starting materials were dissolved in a water/HCl solution and poured into the hydrothermal reactor for 12 hours at 180 ˚C. After the completion of the reaction the obtained solution was placed in the dark at room temperature to obtain the crystal of molecular fluorophore.

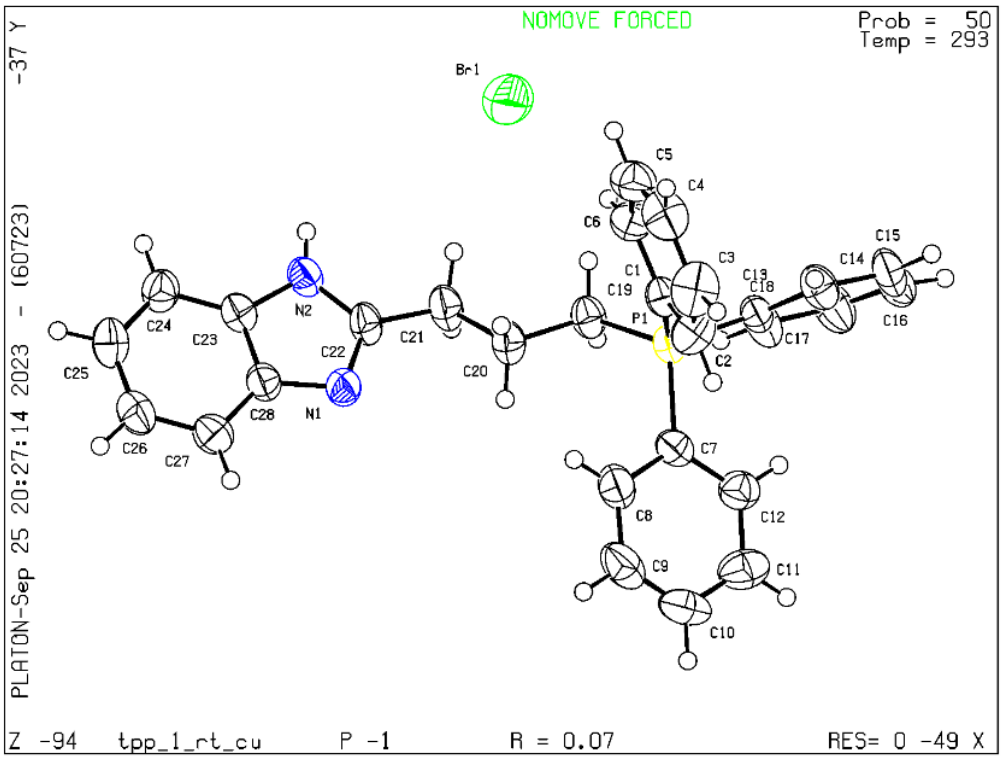

Figure S11: ORTEP diagram of molecular fluorophore with the atom-numbering. Displacement ellipsoids are drawn at the 50% probability level and H atoms are shown as small spheres of arbitrary radius.

Table S1: Crystal data and structure refinement for Molecular Fluorophore

Compound	Molecular fluorophore
Identification code	TPP_1_Rt_Cu
Empirical Formula	$C_{28}H_{26}BrN_2P$
Formula Weight	501.39
T/K	293
Crystal System	Triclinic
Space group	P-1
a (Å)	9.3359(5)
b (Å)	11.3294(8)
c (Å)	13.5336(9)
α (°)	99.456(6)
β (°)	104.083(5)
γ (°)	91.381(5)
V ($Å^3$)	1366.48(16)
Z	2
Density gm/cm3	1.219
μ/mm^{-1}	2.717
F (000)	516.0
Crystal size/mm^3	0.419 × 0.264 × 0.182
Radiation	Cu Kα (λ = 1.54184)
2**Θ** range for data collection/°	7.93 to 132.446
Index range	$-11 \leq h \leq 10, -13 \leq k \leq 13, -15 \leq l \leq 16$
Reflections collected	8752
Independent reflections	4290 [Rint = 0.0357, Rsigma = 0.0384]
Data/restraints/parameters	4290/0/289
Goodness-of-fit on F^2	1.046
Final R indexes [I>=2σ (I)]	R_1 = 0.0671, wR_2 = 0.1883
Final R indexes [all data]	0.0775, 0.2021
Largest diff. peak/hole/e $Å^{-3}$	0.95/-1.28

Experimental details of Molecular Fluorophore

Single crystals of $C_{28}H_{26}BrN_2P$ **[TPP_1_Rt_Cu]**; Single crystal X-ray diffraction data of Fluorophore were collected on an Agilent SuperNova diffractometer, equipped with multilayer optics, monochromatic dual source (Cu and Mo), and Eos CCD detector. The crystal was kept at 293 K during data collection. Using Olex2 [2], the structure was solved with the SHELXT [3] structure solution program using Direct Methods and refined with the SHELXL [3] refinement package using Least Squares minimization. The Solvent-Masking procedure as implemented in Olex2 was used to remove the contribution of some 74 electrons of disordered solvent molecules from the refinement.

Crystal structure determination of Molecular Fluorophore : Crystal Data for $C_{28}H_{26}BrN_2P$ (*M* =501.39 g/mol): triclinic, space group P-1 (no. 2), *a* = 9.3359(5) Å, *b* = 11.3294(8) Å, *c* =

13.5336(9) Å, α = 99.456(6)°, β = 104.083(5)°, γ = 91.381(5)°, V = 1366.48(16) Å^3, Z = 2, T = 293 K, μ(Cu Kα) = 2.717 mm^{-1}, *Dcalc* = 1.219 g/cm^3, 8752 reflections measured (7.93° ≤ 2Θ ≤ 132.446°), 4290 unique (R_{int} = 0.0357, R_{sigma} = 0.0384) which were used in all calculations. The final R_1 was 0.0671 (I > 2σ(I)) and wR_2 was 0.2021 (all data).

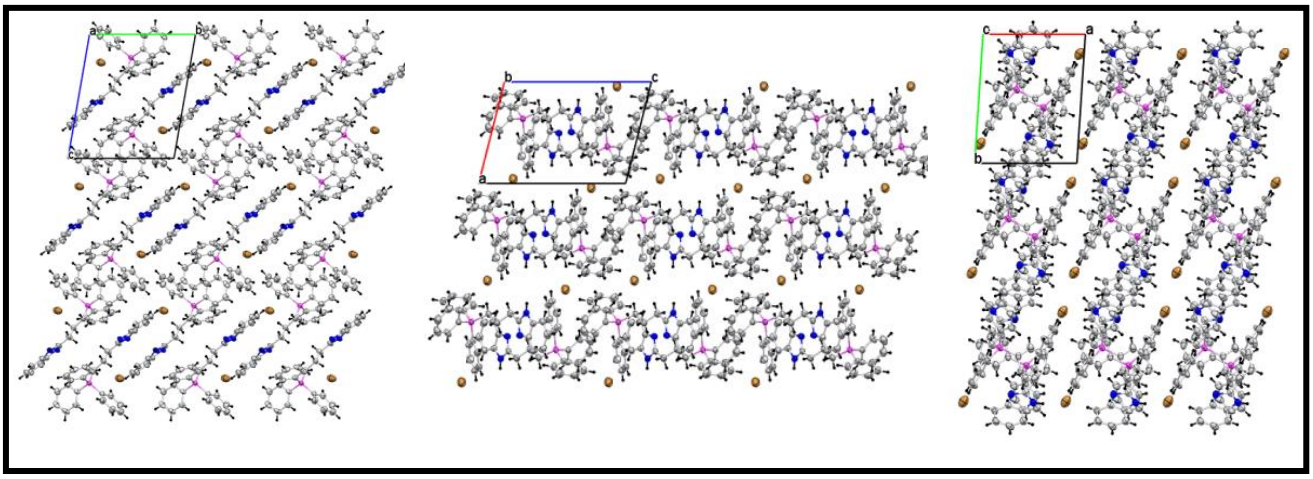

Fig. S12: Crystal packing diagram of fluorophore $C_{28}H_{26}N_2P^+Br^-$along the a, b, and c-axis.

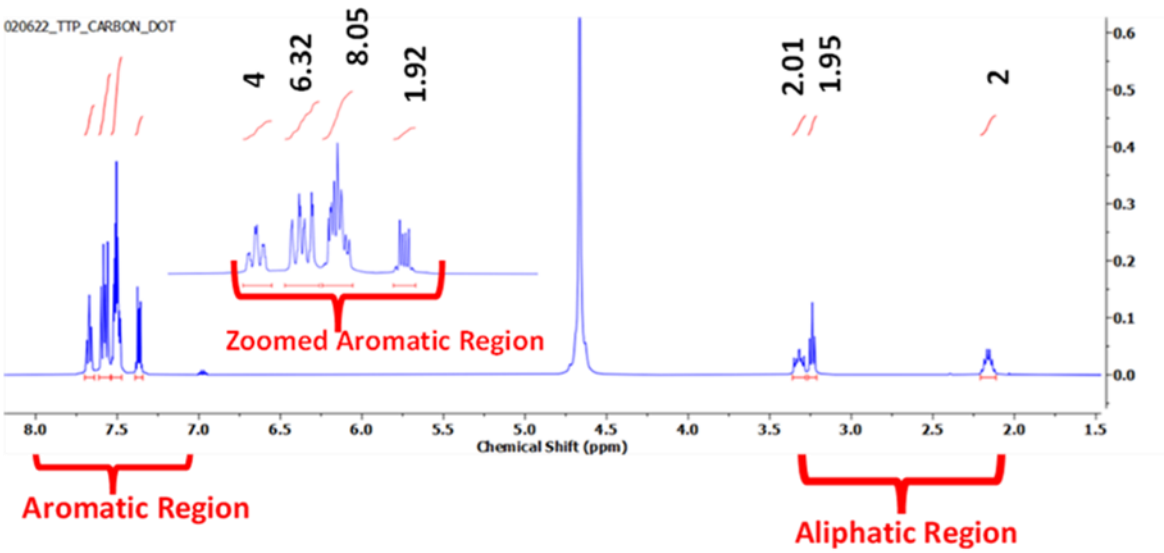

Fig. S13: ^{1}H NMR spectra confirmed the structure of Molecular Fluorophore $C_{28}H_{26}N_2P^+Br^-$. The ^{1}H-NMR spectroscopy reveals the presence of additional protons in the aromatic region at 7.65 and 7.35 ppm, thus suggesting the cyclization between TPP and OPDA while the absence of a peak at 12.02 ppm corresponding to carboxylic hydrogen confirms the structure of MF.

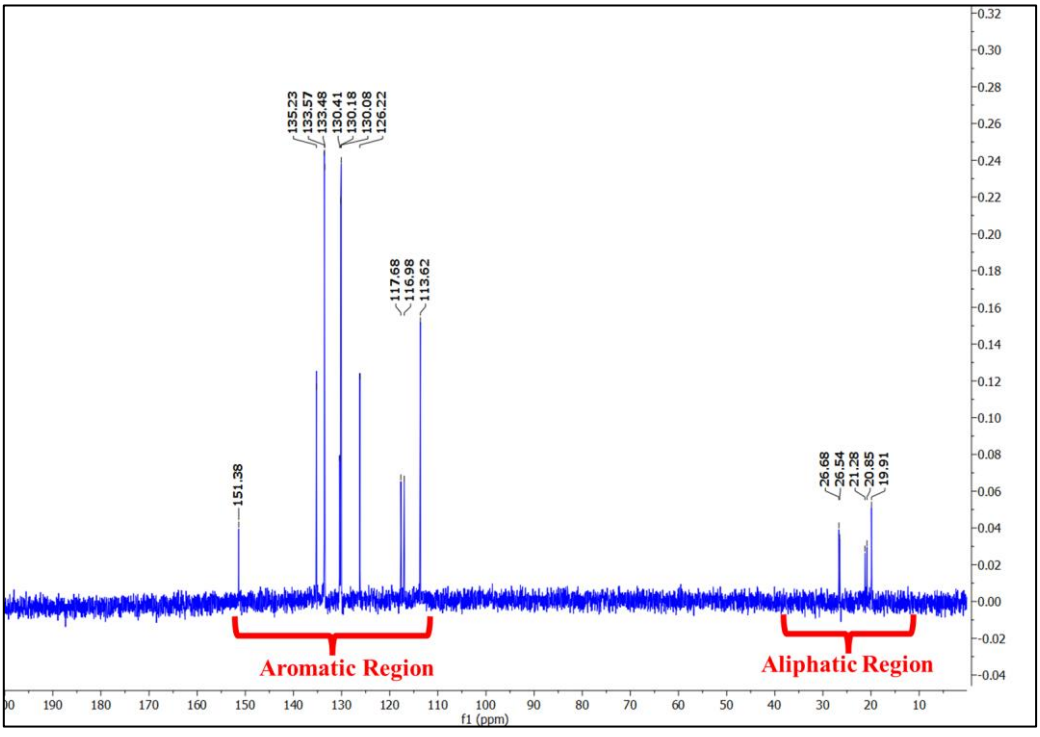

Fig. S14: ^{13}C NMR spectra of fluorophore $C_{28}H_{26}N_2P^+Br^-$. ^{13}C-NMR spectroscopy also reveals the formation of MFs due to the generation of new peak values at 151.38, 135.23, 117.68, and 113.62 ppm, which were absent in the TPP molecule.

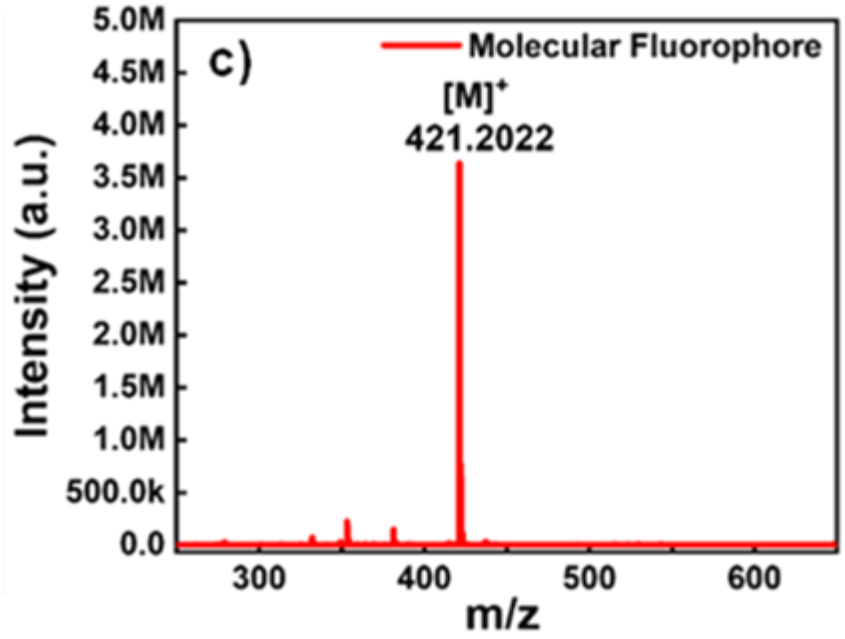

Fig. S15: Mass spectra confirm the presence of molecular fluorophore,

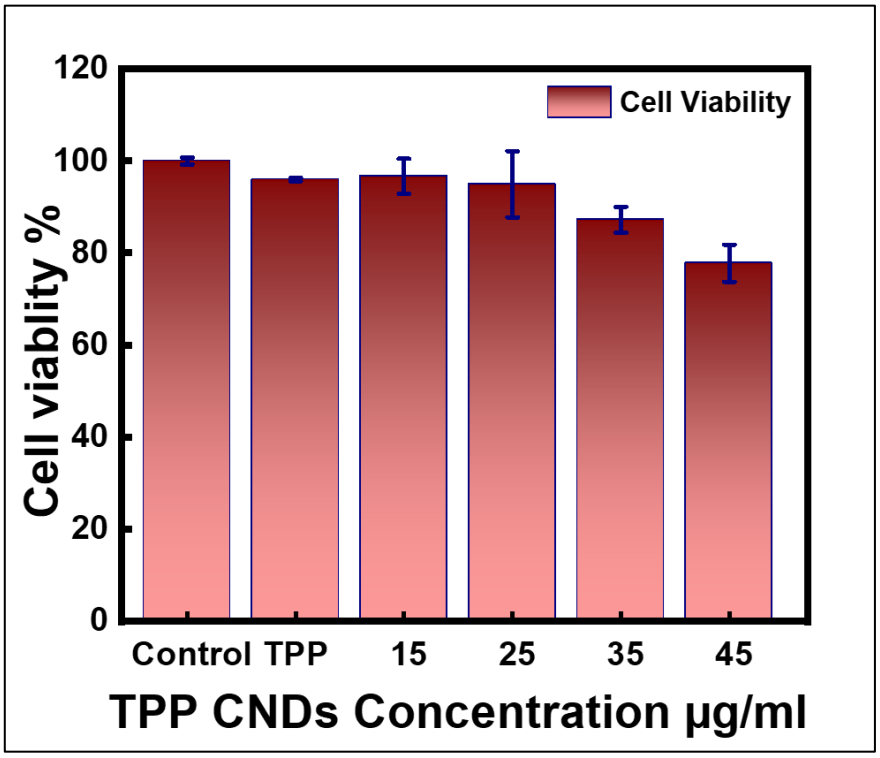

Fig. S16: Cell Viability of HeLa cells after treatment with different concentrations of TPP CNDs.

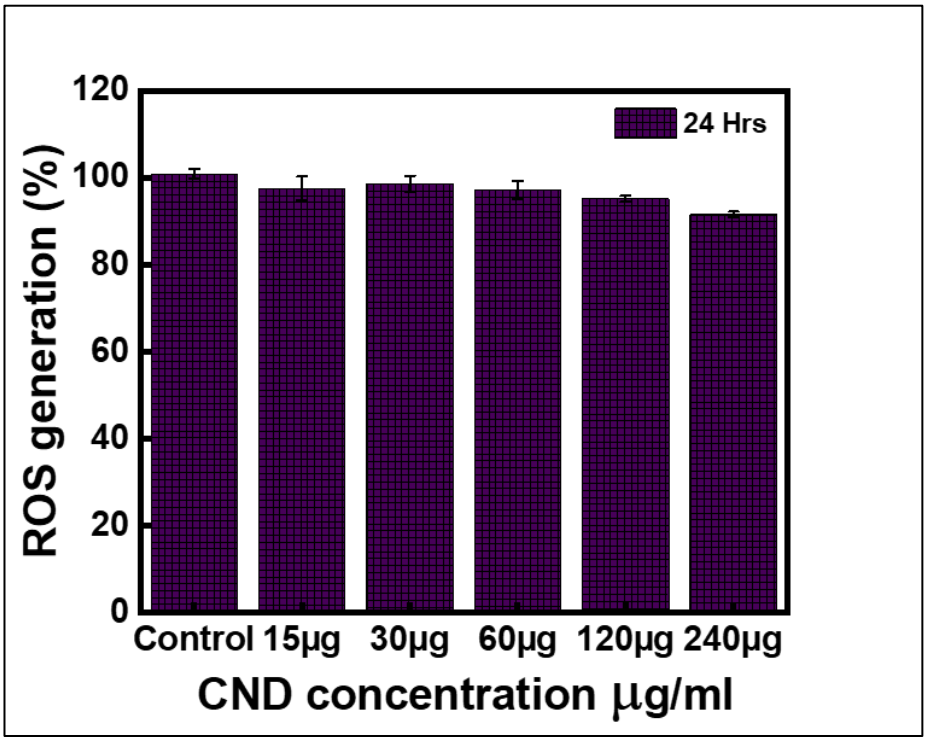

Fig. S17: ROS generation identification with different concentrations of TPP CNDs. A minimum ROS production was observed.

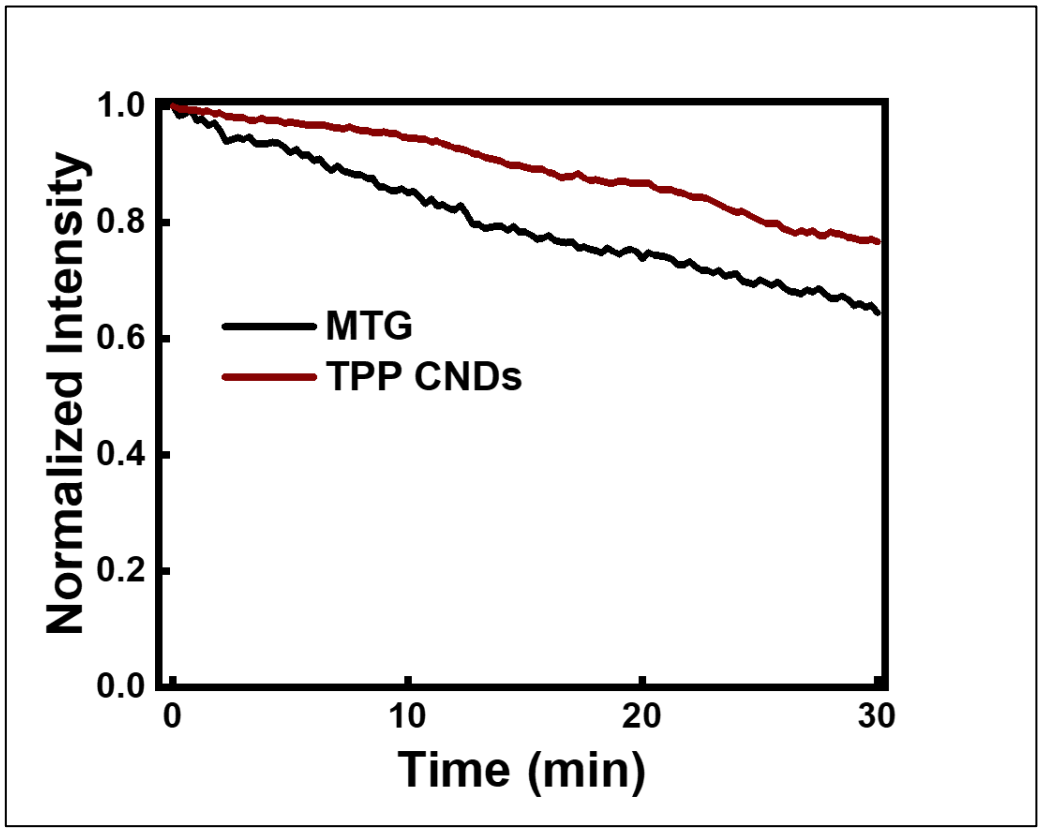

Fig. S18: Photostability of TPP CNDs and MitoTracker Green. The TPP CNDs were found to be more photostable than MitoTracker Green.

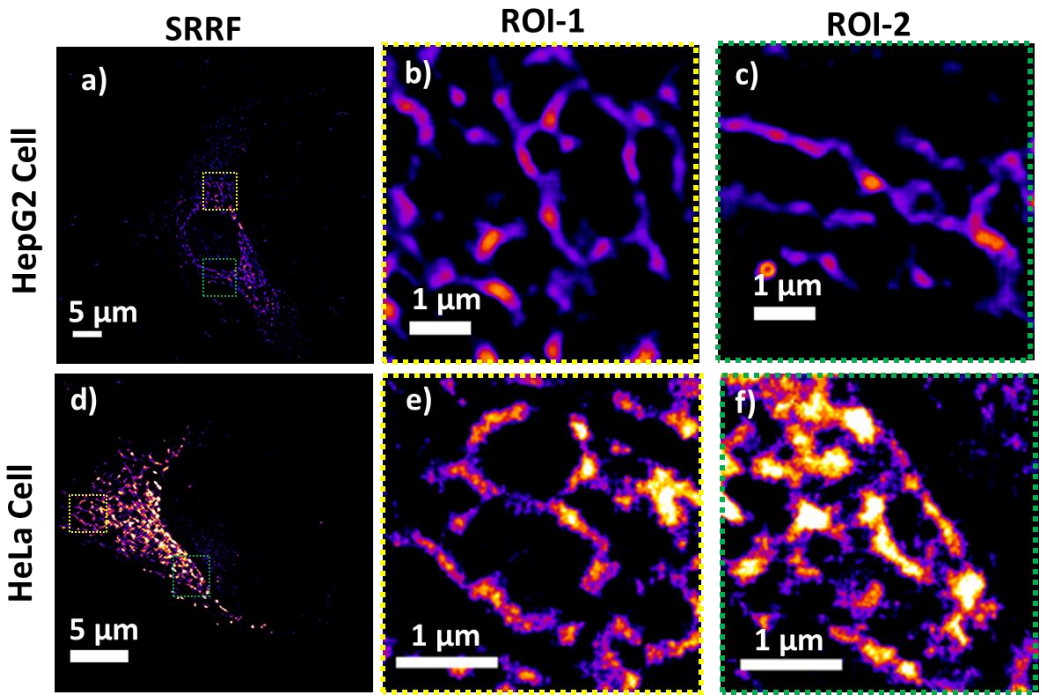

Fig. S19: SRRF images of mitochondria in HepG2 and HeLa cells stained TPP CNDs, (a and d) SRRF images of mitochondria in HepG2 cells and HeLa cells, **(b, c, e, and f)** are the zoomed images of the region of interest of figure a and d. A nice filamentous structure of mitochondria was observed.

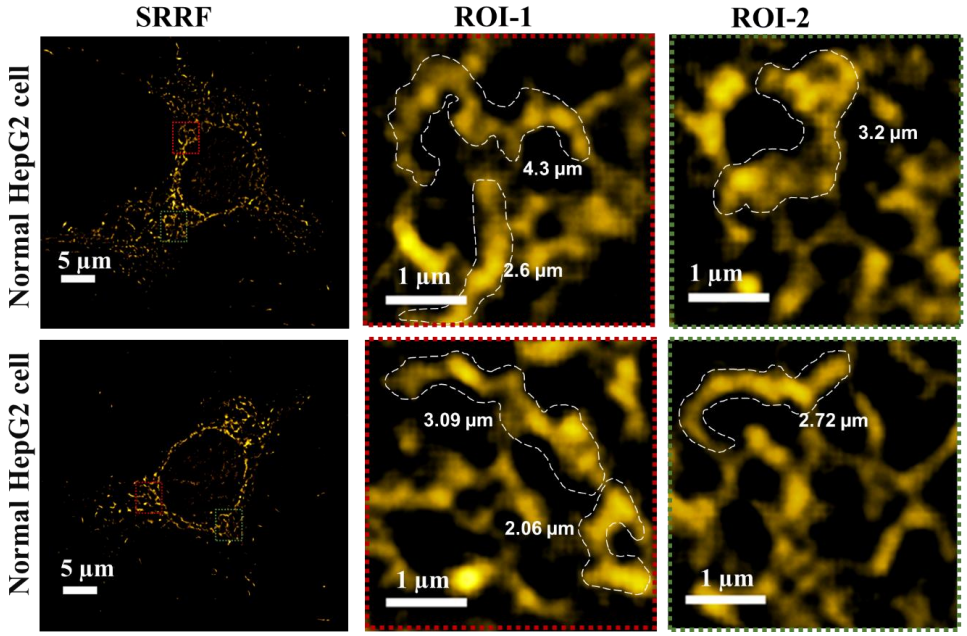

Fig. S20: SRRF images of mitochondria in normal HepG2 cells.

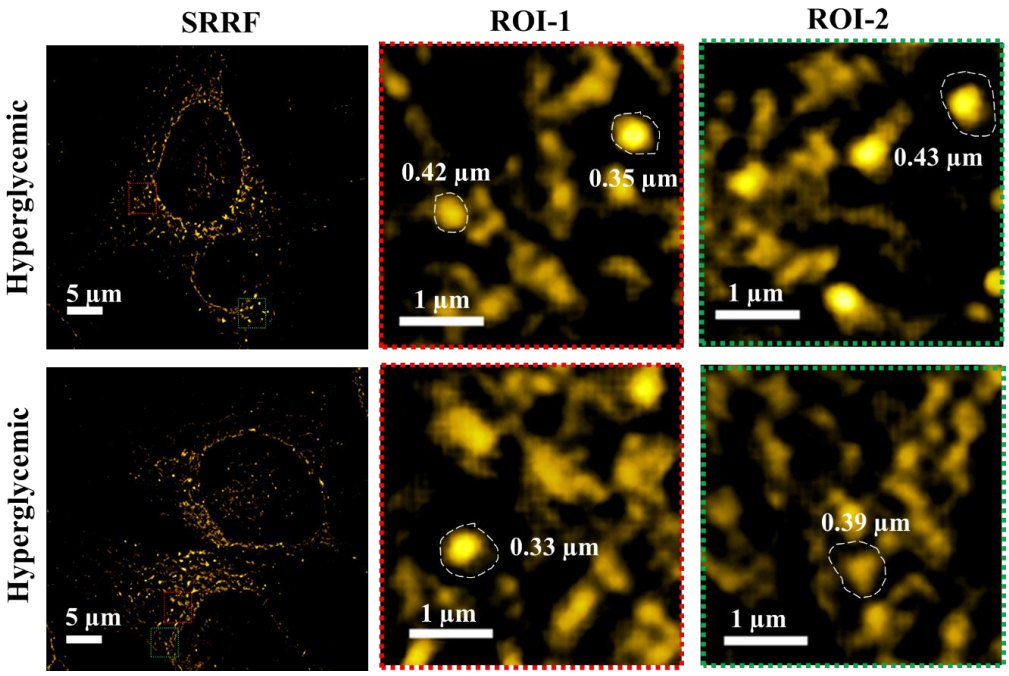

Fig. S21: SRRF images of mitochondria in hyperglycemic HepG2 cells.

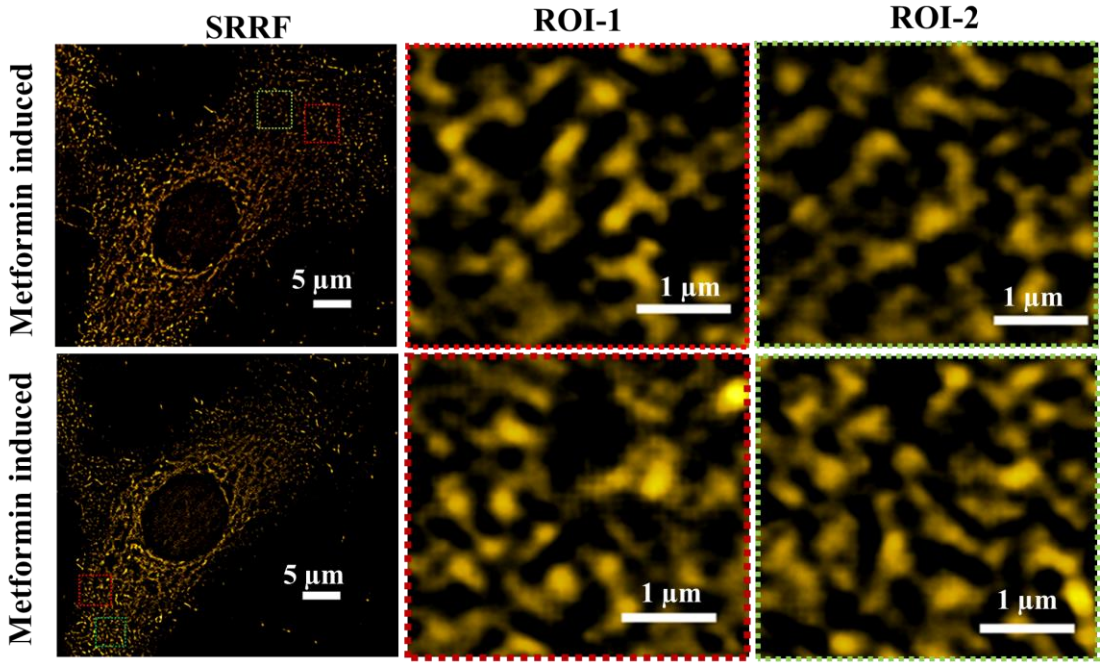

Fig. S22: SRRF images of mitochondria in Metformin exposed HepG2 cells.

References:

1. C. M. Palmeira, A. P. Rolo, J. Berthiaume, J. A. Bjork and K. B. Wallace, *Toxicol. Appl. Pharmacol.*, 2007, **225**, 214–220.
2. O. V. Dolomanov, L. J. Bourhis, R. J. Gildea, J. A. K. Howard and H. Puschmann, *J. Appl. Crystallogr.*, 2009, **42**, 339–341.
3. G. M. Sheldrick, *Acta Crystallogr. Sect. A Found. Adv.*, 2015, **71**, 3–8.